Applied Microscopy
Korean Society of Microscopy

pISSN 2287-5123 · eISSN 2287-4445
https://doi.org/10.9729/AM.2017.47.3.110

Regular Article

Evaluation of Kinetic Parameters and Thermal Stability of Melt-Quenched Bi_xSe_{100-x} Alloys (x ≤7.5 at%) by Non-Isothermal Thermogravimetric Analysis

Mais Jamil A. Ahmad, Mousa M. Abdul-Gader Jafar[1,*], Mahmoud H. Saleh[2], Khawla M. Shehadeh[1], Ahmad Telfah, Khalil A. Ziq[3], Roland Hergenröder

Leibniz Institut für Analytische Wissenschaften–ISAS e.V., Dortmund 44139, Germany
[1]Department of Physics, Faculty of Science, The University of Jordan, Amman 11942, Jordan
[2]Department of Physics and Basic Sciences, Faculty of Engineering Technology, Al-Balqa Applied University, Amman 11134, Jordan
[3]Physics Department, King Fahd University of Petroleum and Minerals, Dhahran 31261, Saudi Arabia

*Correspondence to:
Jafar MMA-G,
Tel: +00962-6-5355000-22042
Fax: +00962-6-5300253
E-mail: mousa_jafar_2030@yahoo.com

Received June 7, 2017
Revised September 1, 2017
Accepted September 1, 2017

Non-isothermal thermogravimetry (TG) measurements on melt-quenched Bi_xSe_{100-x} specimens (x=0, 2.5, 7.5 at%) were made at a heating rate β=10°C/min in the range T=35°C~950°C. The as-measured TG curves confirm that Bi_xSe_{100-x} samples were thermally stable with minor loss at $T \lesssim 400$°C and mass loss starts to decrease up to 600°C, beyond which trivial mass loss was observed. These TG curves were used to estimate molar (Se/Bi)-ratios of Bi_xSe_{100-x} samples, which were not in accordance with initial composition. Shaping features of conversion curves $\alpha(T)$–T of Bi_xSe_{100-x} samples combined with a reliable flow chart were used to reduce kinetic mechanisms that would have caused their thermal mass loss to few nth-order reaction models of the form $f[\alpha(T)] \propto [1-\alpha(T)]^n$ (n=1/2, 2/3, and 1). The constructed $\alpha(T)$–T and $(d\alpha(T)/dT)$–T curves were analyzed using Coats-Redfern (CR) and Achar-Brindley-Sharp (ABS) kinetic formulas on basis of these model functions, but the linearity of attained plots were good in a limited $\alpha(T)$–region. The applicability of CR and ABS methods, with model function of kinetic reaction mechanism R0 (n=0), was notable as they gave best linear fits over much broader $\alpha(T)$-range.

Key Words: Non-isothermal kinetics, Thermogravimetric analysis, Coats-Redfern kinetic model, Achar-Brindley-Sharp kinetic model, Bismuth-selenium alloys

INTRODUCTION

Undoped amorphous selenium (α-Se) is a twofold-coordinated glassy p-type semiconductor with high dark electrical resistivity (~10^{12} Ω cm at 300 K) and bandgap energy E_g as large as 2 eV at 300 K (Bettsteller et al., 1993; Jafar et al., 2016; Mott & Davis, 1979; Saleh et al., 2017). Yet, undoped α-Se has minor photosensitivity for electromagnetic radiation of red wavelengths and larger (Bettsteller et al., 1993; Jafar et al., 2016; Mott & Davis, 1979). In addition, unwanted thermal-/photo- crystallization features of pure a-Se at low ambient temperatures, due to its low glass-transition temperature T_G (around 45°C), make it of unstable structure and short working lifetime arising from ageing effects and thermal instability that lead to adverse changes in its physical properties (Innami & Adachi, 1999; Kasap et al., 1990; Saleh et al., 2017; Tonchev & Kasap, 2002). A practical approach that may enhance photosensitivity of α-Se to long-wavelength light, besides reducing its ageing features, improving its thermal stability and reforming its structure for use in various technical applications, is to alloy it with the other chalcogens (tellurium [Te] or sulfur [S]) and/or with metallic/non-metallic elements to form binary (or ternary) Se-based chalcogenide glasses (Kasap & Rowlands,

2000; Kotkata et al., 2009; Mehra et al., 1993; Mehta, 2006; Mott & Davis, 1979; Saxena & Bhatnagar, 2003). Among the materials which have been alloyed with Se, metallic Bi has peculiar significant influence upon optical, electrical and thermal characteristics of the α-Se semiconductor, with glassy, homogeneous chalcogenide Bi_xSe_{100-x} composites of small Bi-contents (x<10 at%) are still electrically resistive, besides their favorably physical properties that are expedient for many applications of technological curiosity, especially when these Bi_xSe_{100-x} chalcogenides are used to produce thin/thick films for photovoltaic systems and memory devices (Abdel-Rahim et al., 2008; Abu El-Oyoun, 2000; Ahmad, 2016; Atmani, 1992, 1988; Atmani & Vautier, 1989; Atmani et al., 1989; Hafiz et al., 2001; Moharram & Abu El-Oyoun, 2000; Tichy et al., 1985).

A few number of studies related to glass formation, crystallization behavior and melting characteristics of melt-quenched Bi_xSe_{100-x} ingots (Abdel-Rahim et al., 2008; Abu El-Oyoun, 2000; Moharram & Abu El-Oyoun, 2000) and of flash-evaporated Bi_xSe_{100-x} layers (Atmani, 1988; Atmani & Vautier, 1989; Atmani et al., 1989) have been conducted by the differential scanning calorimetry (DSC) and differential thermal analysis (DTA) techniques (Brown, 2004). Not much work is reported on the stoichiometry of melt-quenched Bi_xSe_{100-x} alloys or on their thermogravimetric (TG) behavior, in particular (Ahmad, 2016). Thermogravimetric analysis (TGA) (Brown, 2004; Keattch & Dollimore, 1975; Moukhina, 2012; Šesták, 1984) yields valuable information on the thermal stability of a substance and on activation energy of decomposition processes of samples upon heating, besides using the as-measured TG curves to calculate its chemical composition and differential thermogravimetric (DTG) curves. In this work, we shall study the TG/DTG features of melt-quenched Bi_xSe_{100-x} alloys with various Bi-contents (x=0, 2.5, and 7.5 at%) to examine their homogeneity, chemical composition and thermal stability to acquire some idea about the proper temperature for fabricating stoichiometric Bi_xSe_{100-x} films. Also, the TG/DTG data will be analyzed by model-based integral and differential kinetic formulas as provided by Coats-Redfern (CR) (Coat & Redfern, 1964) and Achar-Brindley-Sharp (ABS) (Achar et al., 1966).

MATERIALS AND METHODS

Thermogravimetry and Kinetic Analysis Methods

TG is an effective thermoanalytical technique that measures the loss of mass m of a material as a function of time t (isothermal or constant-temperature mode) or as a function of sample's temperature T (non-isothermal mode) in a temperature-controlled atmosphere (Brown, 2004; Keattch & Dollimore, 1975; Moukhina, 2012; Šesták, 1984). The TG measurements can be used to estimate chemical composition of sample and predict its thermal stability up to elevated temperatures. The TG technique characterizes substances exhibiting mass loss upon thermal heating due to a variety of thermal mechanisms such as dehydration and desorption, oxidation and absorption, physical evaporation, sublimation and decomposition. Quantitative kinetic analysis methods are concerned with the determination of the activation energy E_α and frequency factor A of underlying kinetic reaction mechanisms. Generating DTG or isoconversional curves from TG measurements as a function of time t at fixed T or T at different constant heating rates will be helpful for a full kinetic analysis (Moukhina, 2012; Šesták, 1984).

Model-based Kinetic Methods for Quantitative Analysis of TG and DTG Data

Quantitative analysis of as-measured TG curves of a sample and their DTG curves, which index the point at which mass loss is prominent, can yield valuable information on the kinetic processes associated with the observed thermal mechanisms occurring in the sample. Yet, the TG/DTG curves are not "fingerprint" curves of the material in the sense that thermal mechanisms are kinetic in nature—that is, there is a reaction rate at which they occur. The rate at which a kinetic process proceeds depends not only on the temperature T it is at, but also on the time t it has spent at that T; thus, any experimental parameter that can affect the reaction rate of a thermal process in a sample will lead to change in the shape of TG/DTG curves and transformation temperatures. These parameters include the material type, shape and size of the sample's pan, ramp rate, as well as the type of the gas (inert or oxidizing gas) purged into the TG-instrument chamber and mass/volume of the sample, besides its form and morphology (Brown, 2004; Keattch & Dollimore, 1975; Šesták, 1984). A change in the temperature T_0 at which decomposition commences in TG curves and a shift in the peak temperature T_p of DTG curves are supposed to be affected by varying sample mass m and heating rate $\beta=dT/dt$. Improving resolution of non-isothermal TG measurements and separating possible thermal processes can be realized via long experimental runs at slow heating rates (2°C/min~30°C/min), so the time at any T must be long enough to permit completeness of a kinetic reaction, by reducing sample's size (5~30 mg), hence minimizing temperature gradients and inhomogeneities across it, and by choosing a suitable purge gas during TG measurements.

As regards to kinetic analysis of experimental thermoanalytical data, two main approaches are realized: the model-free and model-based analysis methods, both demand a set of accurate isothermal or non-isothermal measurements at different conditions, such as the sample's temperature T and the heating rate β (Abdel-Rahim et al., 2008; Abu El-Oyoun, 2000; Achar et al., 1966; Atmani, 1988; Atmani & Vautier, 1989; Atmani et al., 1989; Brown, 2004; Coat &

Redfern, 1964; Flynn & Wall, 1966; Jones et al., 1975; Keattch & Dollimore, 1975; Marini et al., 1979; Moharram & Abu El-Oyoun, 2000; Moukhina, 2012; Ozawa, 1965; Ptáček et al., 2010; Šesták, 1984; Sharp & Wentworth, 1969; Sharp et al., 1966). The model-based kinetic (discrimination) analysis solves an equation (Eq.) based on a given kinetic model function $f[\alpha(t)]$ or $f\{\alpha[T(t)]\}$ that would describe the underlying kinetic process operative in the heated sample and allow the determination of its activation energy E_α, where $\alpha(t)$ or $\alpha[T(t)]$ is the conversion factor characterizing such kinetic process at the time t or temperature T. The model-free methods use the data of a series of non-isothermal TG curves at different heating rates to determine E_α of the kinetic reaction mechanism responsible for the sample's thermal behavior but do not provide useful information about the kinetic model $f\{\alpha[T(t)]\}$ describing it.

In non-isothermal TG measurements, $\Delta m\%=[(m[T/(t)]/m_i)\times 100]\%$, the percentage ratio of the sample's mass $m[T(t)]$ at the temperature $T(t)$ to its initial mass m_i, is customarily recorded. The non-isothermal DTG curve of a heated sample is the first derivative of the measured $\Delta m\%-T(t)$ curve with respect to $T(t)$—that is, $\mathrm{d}(\Delta m\%)/\mathrm{d}T$. To analyze non-isothermal TG/DTG data, the fraction $\alpha[T(t)]$ of the sample decomposed at $T(t)$ is needed. The first derivative of $\alpha[T(t)]$ with respect to t is $\mathrm{d}\alpha[T(t)]/\mathrm{d}t=[\mathrm{d}\alpha[T(t)]/\mathrm{d}T][\mathrm{d}T(t)/\mathrm{d}t]=\theta(t)[\mathrm{d}\alpha[T(t)]/\mathrm{d}T]$, where $\theta(t)$ is the time rate of heating. For a linear heating ramp $T(t)=T_{start}+\beta t$, $\theta(t)$ is a constant heating rate β, where T_{start} is the temperature at which TG measurements started. For $\alpha[T(t)]$ to be in the range 0 to 1, we define it in terms of measured quantities $W[T(t)=\Delta m\%/100$ and $W_f=[(m_f/m_i)\%]/100$ as

$$\alpha[T(t)]=\frac{m_i-m[T(t)]}{m_i-m_f}=\frac{1-W[T(t)]}{1-W_f} \tag{1}$$

where m_f is the residual mass of sample remains at the end of a thermal decomposition process. The rate of reaction conversion $\mathrm{d}\alpha[T(t)]/\mathrm{d}T$ can then be described, for a constant heating rate β, by the expression

$$\frac{\mathrm{d}\alpha[T(t)]}{\mathrm{d}T}\equiv\frac{\mathrm{d}\left[\frac{1-W[T(t)]}{1-W_f}\right]}{\mathrm{d}T}=-\left(\frac{1}{1-W_f}\right)\frac{\mathrm{d}W[T(t)]}{\mathrm{d}T}=-\left(\frac{1}{1-W_f}\right)\left(\frac{\mathrm{d}W[T(t)]}{\mathrm{d}t}\right)\frac{1}{\beta}. \tag{2}$$

Eq. (2) can be used to construct a curve of $\mathrm{d}\alpha[T(t)]/\mathrm{d}T$–$T(t)$ by numerical differentiation of the $\alpha[T(t)]$–$T(t)$ data.

Model-based (discrimination) kinetic analysis methods include the differential-form method of ABS (Achar et al., 1966) and integral-form method proposed by CR (Coat & Redfern, 1964), which was amended by Marini et al. (1979) to extend its applicability to a broader range of $\alpha(t)$ or $\alpha[T(t)]$ values. We shall give the key algebraic formulas of these model-based CR and ABS methods, which can be employed to analyze non-isothermal TG/DTG curves at a constant heating rate $\beta=\mathrm{d}T/\mathrm{d}t$ using the model function $f[\alpha(T)]\propto[1-\alpha(T)]^n$ for few values of the reaction order (n=0, 1/2, 2/3, and 1) (Marini et al., 1979; Sharp & Wentworth, 1969). Having the conversion curves or the $\mathrm{d}\alpha(T)/\mathrm{d}T$-$T$ data, calculated from non-isothermal TG curve at a constant β using a kinetic model function $f[\alpha(T)]=\gamma\,[1-\alpha(T)]^n$, where γ is a numerical constant, depends on the kinetic reaction mechanism, the model-based differential-form ABS analysis method has the form (Achar et al., 1966; Marini et al., 1979)

$$\ln\left\{\frac{1}{\gamma[1-\alpha(T)]^n}\frac{\mathrm{d}\alpha(T)}{\mathrm{d}T}\right\}=\ln\left(\frac{A}{\beta}\right)-\frac{E_a}{RT}\,. \tag{3}$$

For a fixed reaction order n, a plot of $\ln\{(\mathrm{d}\alpha(T)/\mathrm{d}T)/(\gamma[1-\alpha(T)]^n)\}$ as a function of $1/T$ at a single constant $\beta=\mathrm{d}T/\mathrm{d}t$, where T (in K) is the sample's temperature, may display a straight-line portion, to which a linear regression can be applied over some range of $\alpha(T)$ values to determine directly the activation energy E_α (its slope) and frequency factor A (its intercept), both are presumed to be constants, independent of T, that are related to the kinetic reaction mechanism operating in the sample in that region of $\alpha(T)$. The model-based integral-form CR kinetic method, combined with an nth-order model function $f[\alpha(T)]=\gamma[1-\alpha(T)]^n$, can also be employed to analyze conversion curves of a substance calculated from non-isothermal TG curves measured at a constant β. The CR-formula can be expressed for the kinetic reaction nth-order model function $f[\alpha(T)]$ as (Coat & Redfern, 1964; Marini et al., 1979)

$$\ln\left\{\frac{g[\alpha(T)]}{T^2}\right\}=\mathrm{Ln}\left(\frac{AR}{\beta E_a}\right)-\frac{E_a}{RT}\quad;\quad g[\alpha(T)]=\int_0^{\alpha(T)}\frac{\mathrm{d}\alpha'}{f[\alpha'(T)]}=\int_0^{\alpha(T)}\frac{\mathrm{d}\alpha'}{\gamma[1-\alpha'(T)]^n}\,. \tag{4}$$

The function $g[\alpha(T)]$ of the nth-order model function $f[\alpha(T)]=\gamma[1-\alpha(T)]^n$ can be expressed as

$$g[\alpha(T)]=\int_0^{\alpha(T)}\frac{\mathrm{d}\alpha'}{\gamma\left(1-\alpha'\right)^n}=\begin{cases}[1-[1-\alpha(T)]^{1-n}]/[\gamma(1-n)] & \text{if } n\neq 1\\ \{-\ln[1-\alpha(T)]\}/\gamma & \text{if } n=1\end{cases}. \tag{5}$$

A plot of $\ln\{g[\alpha(T)]/T^2\}$–$1/T$(K) for a constant heating rate β gives a straight line over a range of $\alpha(T)$ if an nth-order model function $f[\alpha(T)]$ and its integral function $g[\alpha(T)]$ are adequately selected. The slope and intercept of a least-squares fit to the data of the linear portion yield E_α and A, respectively. Among several other approaches (Criado et al., 1989; Perez-Maqueda et al., 1996), the features of TG/DTG curves can be used to quest for probable kinetic reaction mechanisms responsible for the substance's thermal decomposition in a certain temperature range. Few tactics were proposed

for choosing the reaction model that describes a thermal process in the sample upon non-isothermal heating on the basis of its asymmetry or shape of DTG curves via few characteristic parameters (Dollimore et al., 1992a, 1992b; Gao et al., 1993; Haixiang et al., 2010; Lee & Dollimore, 1998). These parameters include the initial temperature T_i, where mass loss commences and the final temperature T_f, where no mass loss takes place, which on the DTG curves are often termed as diffuse (d) or sharp (s), depending on the decrease/increase slanting of the conversion rate. Other parameters are experimental conversion factor at maximum rate (α_m^{exp}) of the reaction process—that is, the value of $\alpha(T)$ at temperature Tm corresponding to the peak (maximum) of the DTG curve, and half width $\Delta_{1/2}^{exp} \equiv T_2 - T_m$ or the width on the $d\alpha(T)/dT$–T curve at half height measured between the temperatures T_1 and T_2 (Haixiang et al., 2010). Some kinetic mechanisms lead to asymptotic or "diffuse" departure from base line of a DTG curve, while others produce "sharp" slant to the final TG/DTG plateau (Dollimore et al., 1992a, 1992b; Gao et al., 1993; Haixiang et al., 2010; Lee & Dollimore, 1998).

The asymmetry of a DTG curve can be labeled by an asymmetry (shape) factor $S=\alpha/b$, with $\alpha=T_m-T_1$ and $b\equiv T_2-T_m$ (Dollimore et al., 1992a, 1992b; Gao et al., 1993; Lee & Dollimore, 1998), so $S\approx1$ for kinetic mechanisms of DTG curves with both T_i and T_f sharp (or diffuse) and $S<1$ for DTG curves with T_i sharp and T_f diffuse. But $S>1$ for DTG curves with "slow" departure from base line (T_i diffuse) and with a "fast" return to the base line (T_f sharp), for which we can disregard kinetic processes of first-order model functions; thus, visual inspection of the asymmetry of a DTG trace and its shaping features may help to limit kinetic mechanisms to favorite ones (Dollimore et al., 1992a, 1992b; Gao et al., 1993; Haixiang et al., 2010; Lee & Dollimore, 1998).

The values of α_m^{exp} and $\Delta_{1/2}^{exp}$ can be compared with predicted values of maximum conversion α_m^{theor} and half width $\Delta_{1/2}$ via constructing DTG curves for diverse sets of the reaction "kinetic triplet": E_α, A and $f[\alpha(T)]$ that should characterize a unique solid state reaction, and then use a plausible shape method or flow chart (Haixiang et al., 2010) to further identify the more favored mechanism of thermal decomposition of a solid. A shape method (flow chart) is recently proposed by Haixiang et al. (2010) who obtained analytical expressions for α_m^{theor} and simulated values of $\Delta_{1/2}$ for a non-isothermal dynamic curve (DTG or DSC curve with a constant heating rate $\beta=dT/dt$) for many kinetic model functions $f[\alpha(T)]$ (Criado et al., 1989; Dollimore et al., 1992a, 1992b; Gao et al., 1993; Haixiang et al., 2010; Lee & Dollimore, 1998; Perez-Maqueda et al., 1996), besides giving theoretical limits for α_m^{theor} in range $15 \le x=E_\alpha/RT \le 70$.

In this work, we shall utilize such experimental features to seek kinetic models that may describe the TG/DTG curves of melt-quenched Bi_xSe_{100-x} ingots ($x\le7.5$ at%) and carry out detailed curve fitting of their non-isothermal TG data, measured at $\beta=10$°C/min, to the model-based differential ABS and integral CR analysis methods using the nth-order model function $f[\alpha(T)]=\gamma[1-\alpha(T)]^n$ for n=0, 1/2, 2/3, and 1. The graphical methods and flow charts will be used to identify which kinetic reaction mechanism describes their thermal behavior.

Experimental Details

The melt-quenching method was used to prepare homogeneous chalcogenide Bi_xSe_{100-x} alloys with various Bi-contents (x=0, 2.5, and 7.5 at%) (Ahmad, 2016). In brief, finely-grinded selenium (Se) and bismuth (Bi) powders of the required molar-weight (Bi:Se)-ratios [x:($_{100-x}$)] were mixed thoroughly and placed inside quartz ampoules, which were then evacuated and flushed with high-purity argon (Ar) gas several times before sealing them under 24%-atm Ar-gas. The sealed quartz ampoules were moved to a high-temperature furnace, where they were exposed to thermal heating entailing successive constant 200°C annealing stages, at a heating rate of 60°C/hour, from room temperature up to a temperature lying between 850°C~1,000°C, chosen in accordance with the phase diagrams of Bi-Se alloys and compounds having different molar-(Bi/Se) compositions (Chen et al., 2014; Okamoto, 1994). The {ampoule-Bi_xSe_{100-x} powder}-units were kept at each constant-stage temperature for more than 24 hours, during which they were subjected to mild shivering from time to time to mix their liquid ingredients to ensure homogeneity of the final solid chalcogenide Bi_xSe_{100-x} alloys. After the thermal annealing of quartz ampoules with their contents was completed, the ampoules were quenched directly from the high annealing temperatures into water at room temperature. Details on the preparation procedures and conditions used for producing melt-quenched Bi_xSe_{100-x} alloys of different Bi-contents are described elsewhere (Ahmad, 2016). Small amounts of these Bi_xSe_{100-x} lumps were crushed and finely-grinded and stored in well-covered, humidity-free desiccator for TG measurements to be made on them.

Thermal analysis of Bi_xSe_{100-x} powder samples was achieved by making TG measurements on them using a TG/DSC-equipment (model STA 409 PC Luxx; NETZSCH-Gerätebau GmbH, Germany) to determine their thermal stability and to elucidate the nature of thermal kinetic processes responsible for fractional decomposition of their ingredients, besides estimating their molar chemical compositions. To reduce thermal gradients across the samples on which thermoanalytical measurements to be made, fairly small amounts (≈12~15 mg) of the finely-grinded Bi_xSe_{100-x} powder were uniformly dispersed in the sample's container (an aluminum oxide [Al_2O_3–] pan), installed in the furnace region of the TG instrument, whose reference Al_2O_3-pan was left empty. The sample pan was progressively heated non-isothermally from room temperature, under continuous

purging of pure nitrogen (N_2–) gas at a flow rate of 30 mL/min, up to 950°C at a constant heating rate β=10°C/min. The as-measured TG data were recorded as percentage change of the sample mass $m(T)$, relative to its initial mass m_i, as a function of the furnace temperature T, measured to uncertainty better than ±0.01°C, to obtain a set of Δm%–T data in the selected temperature range, with the DTG data being calculated, smoothed in situ at each temperature $T(t)$ by differentiating the measured TG-data using the PC-software of used TG instrument as $d\Delta m\%/d[T(°C)]$.

RESULTS

Fig. 1 depicts the temperature dependence of as-measured non-isothermal TG and DTG data scanned at β=10°C/min in the range 35°C~950°C, plotted as Δm% and $d\Delta m\%/d[t(\text{min})]$ against the sample's temperature T(°C) for the powder samples of melt-quenched Bi_xSe_{100-x} alloys having x=0, 2.5, and 7.5 at%. Several motivating features can be inferred from these measured TG/DTG curves. No sizeable loss of mass of studied Bi_xSe_{100-x} samples with no signs of desorption (drying), mass gain and/or of thermomolecular flow (convection), can be inferred from their as-measured TG curves at temperatures less than T~ 400°C, below which these Bi_xSe_{100-x} alloys are thermally stable. These features signify that their initial powders were free of water and the nitrogen gas flowing in the chamber of the TG instrument was moisture-free (dry), with no substantial traces of oxidizing gas impurities. The onset (initial) temperature T_i of the mass loss shifts slightly with initial sample's mass that might be related to delay in its thermal decomposition due to temperature gradients across the powder pressed in the pan. At T>400°C, the mass loss starts to decline gradually and then sharply over the temperature window 400°C~600°C, where the DTG curve is seen to slowly ascend till a maximum before it sharply returns to the zero base line.

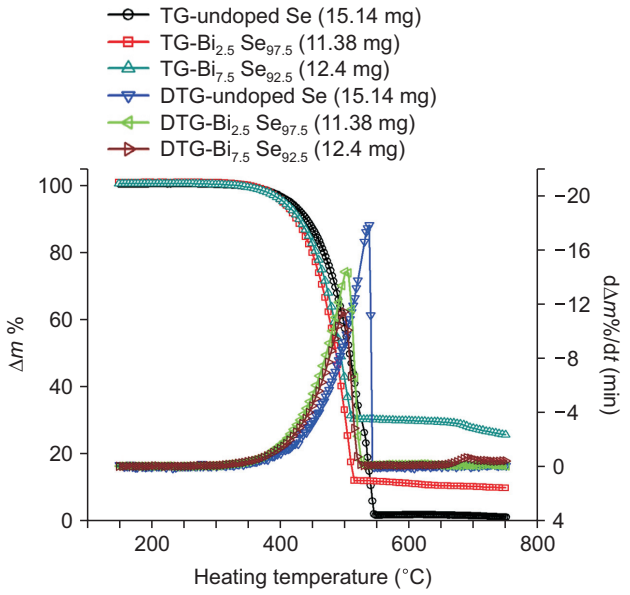

Fig. 1. The as-measured thermogravimetry (TG) curves and calculated differential thermogravimetric (DTG) curves in the temperature range 35°C~950°C for the melt-quenching Bi_xSe_{100-x} alloys having various Bi-compositions.

As T is increased beyond 600°C the mass loss is feeble up to 950°C, with residual mass of Bi_xSe_{100-x} powder may be related to Bi-content used in preparing their melt-quenched Bi_xSe_{100-x} alloys (Ahmad, 2016). This suggests that the observed loss of sample's mass upon thermal heating up to T~600°C may be due to sample's decomposition to its individual elements. This TG/DTG behavior can be realized in view of melting and boiling points of Se (T_{melt}≈220°C and T_{boil}≈685°C) and of bismuth (T_{melt}≈271°C and T_{boil}≈1,564°C) at normal atmospheric pressure. Selenium is more volatile than bismuth and has much higher vapor pressure at temperatures above 300°C, so the drastic decline seen in the studied Bi_xSe_{100-x} samples with rising temperature up to 600°C can be assigned to Se-vaporization from alloy. In the temperature range 650°C~720°C, Fig. 1 shows a slender shoulder/peak on the TG/DTG curves of some of the Bi_xSe_{100-x} powder samples studied (Ahmad, 2016). The origin of existence of such meager shoulder on measured TG/DTG curves is not fully understood.

Presuming that the thermally-heated Bi_xSe_{100-x} powder samples actually suffered from decomposition (breaking apart) into their individual Se- and Bi-components via a certain kinetic reaction mechanism upon increasing the sample's temperature T, one may be able to estimate the chemical composition (stoichiometry) of their as-prepared melt-quenching Bi_xSe_{100-x} alloys from their as-measured Δm%–T(°C) curves. Suppose that the measured percentage of mass loss Δm% of a particular Bi_xSe_{100-x} powder sample down to its shoulder portion at the high-temperature side is totally related to $(\Delta m\%)_{Se}$ and the remainder percentage mass loss is mainly due to the $(\Delta m\%)_{Bi}$ amount. Based on such hypothesis, the stoichiometric (molar) ratios of selenium (M_{Se}=78.96 g/mol) to bismuth (M_{Bi}=208.98 g/mol) estimated from the TG curves of studied Bi_xSe_{100-x} powder samples were not comparable to those initially used in the preparation of their original melt-quenched Bi_xSe_{100-x} alloys, like, for instant, the $Bi_{2.5}Se_{97.5}$ sample. Also, their TG-estimated compositions (Table 1) are not in accord with stoichiometric ratios calculated from spectra acquired by X-ray energy dispersive spectroscopy technique (Ahmad, 2016).

The discrepancy between the (Se-Bi)-ratios estimated from measured TG curves of Bi_xSe_{100-x} samples and those initially mixed to prepare their original melt-quenched Bi_xSe_{100-x} alloys may be partly ascribed to inhomogeneities in melt-

quenched ingots, so the small amounts of powders taken form these ingots for TG characterization might not be well representative of their composition. One had to make TG measurements on powder samples from different parts of ingots, a procedure that we have not carried out in this work; however, this inconsistency might be resolved by the use of accurate analytical spectroscopic techniques such as the X-ray photoelectron spectroscopy (van der Heide, 2012) and X-ray fluorescence spectrometry (Jenkins, 1999), which requires sizable amounts of powder to proceed with composition analysis.

DISCUSSION

Using T_i, T_f, $S=(T_m-T_1)/(T_2-T_m)$, $\Delta^{exp}_{1/2}=(T_2-T_1)$ and $\alpha^{exp}_m = \alpha(T_m)$ and designating features of measured TG/DTG curves of a heated sample, the favored kinetic reaction mechanism responsible for its thermal decomposition can then be identified and discriminated with the help of a flow chart (shape method) that signifies the type and range of these parameters for different kinetic models (Dollimore et al., 1992a, 1992b; Gao et al., 1993; Haixiang et al., 2010; Lee & Dollimore, 1998). Indicative values of these parameters that give a glue on the nature of thermal decomposition of melt-quenching Bi_xSe_{100-x} alloys of the present work were determined by closely visual inspection of the $\alpha(T)$–T in the range $0\leq\alpha(T)\leq1$ and $(d\alpha(T)/dT)$–T of the curves, constructed, using Eqs. 1 and 2, from their measured non-isothermal TG/DTG curves for β=10°C and depicted in Fig. 2. These conversion curves show that initial temperature T_i at which sample's decomposition begins is "diffuse" and final temperature T_f after which decomposition ends is "sharp". Table 2 lists T_m, α^{exp}_m, T_1, T_2, $\Delta^{exp}_{1/2}$ and S, whose values could help to identify favored kinetic reaction mechanisms giving rise to observed thermal decomposition of such alloys. As shape factor $S>1$ and DTG curve is asymmetric for the Bi_xSe_{100-x} alloys, we can disregard some kinetic mechanisms on basis of flow charts and shape methods (Haixiang et al., 2010).

Other irrelevant kinetic reaction models might be further separated and discarded by making use of experimentally-deduced values of the TG/DTG shape parameters $\Delta^{exp}_{1/2}$ and

Table 1. Atomic (Se/Bi)-ratios for the Bi_xSe_{100-x} samples of various Bi-contents obtained from their as-measured thermogravimetry (TG) curves, compared to those initially used to prepare their original melt-quenching Bi_xSe_{100-x} alloys (Ahmad, 2016)

Bi_xSe_{100-x} sample	Atomic (Se/Bi)-ratio	
	TG-estimated	Mixed in original alloy
Bi_0Se_{100}	100	100
$Bi_{2.5}Se_{97.5}$	23.5	39
$Bi_{7.5}Se_{92.5}$	12.4	12.3
$Bi_{10}Se_{90}$	9	6.6
$Bi_{20}Se_{80}$	4	6

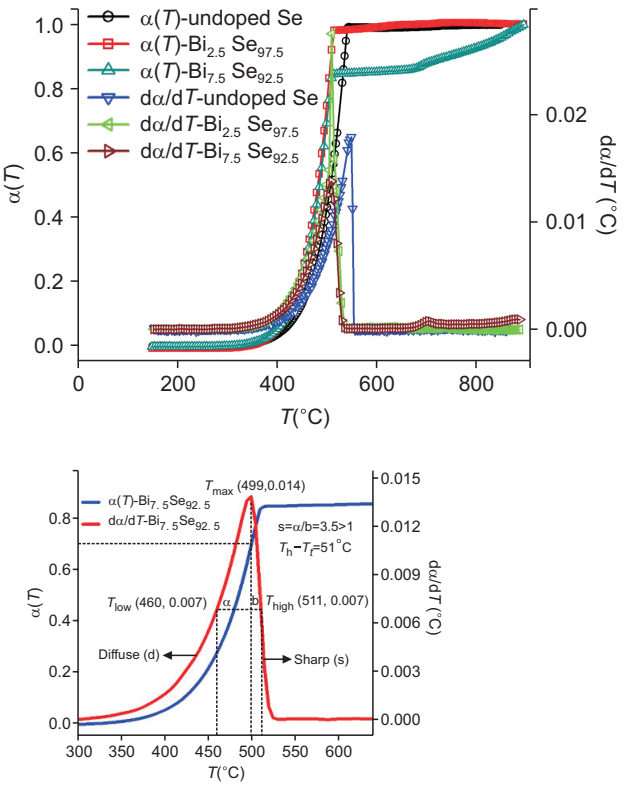

Fig. 2. The $\alpha(T)$–T(°C) and $(d\alpha(T)/dT)$–T(°C) curves for the studied melt-quenching Bi_xSe_{100-x} alloys constructed from their experimental thermogravimetry (TG) and differential thermogravimetric (DTG) curves of Fig. 1 using equations 1 and 2. The inset shows the procedure for selecting some of kinetic model functions responsible for thermal decomposition in the studied samples.

Table 2. Parameters related to characteristic features and asymmetry of $\alpha(T)$–T(°C) and $(d\alpha(T)/dT)$–T(°C) curves for melt-quenched Bi_xSe_{100-x} alloys for β=10°C/min

Bi_xSe_{100-x} sample	T_i (°C)	T_f (°C)	T_m (°C)	T_1 (°C)	T_2 (°C)	$\Delta^{exp}_{1/2}$ (°C)	S	α^{exp}_m
Bi_0Se_{100}	Diffuse	Sharp	538	498	541	43	13.3	0.925
$Bi_{2.5}Se_{97.5}$	Diffuse	Sharp	501	492	509	17	1.13	0.777
$Bi_{7.5}Se_{92.5}$	Diffuse	Sharp	499	461	511	50	3.17	0.662

The meanings of these parameters are given in the text.

α_m^{exp} and of a reliable flow chart, which is generally based on theoretical values of shape parameters that characterize certain kinetic reaction mechanisms whose kinetic parameters E_α and A span a fairly wide range: ($50 \leq E_\alpha \leq 350$ kJ/mol) and $10^5 \leq A \leq 10^{18} s^{-1}$ (Haixiang et al., 2010). In a full kinetic analysis of TG/DTG data, this procedure of model discrimination can be assisted by the application of a non-linear conventional curve-fitting of the $\alpha(T)-T$ and $(d\alpha(T)/dT)-T$ data to the numerous kinetic reaction models to search for the model that would describe the observed thermal decomposition of the sample (Haixiang et al., 2010); however, this is an ad-hoc and unwieldy procedure that only yields reliable and physically-meaning results when a global (not local) minimum solution of the problem is reached. Yet, fairly accurate values of the shape parameters featuring the TG/DTG curves of a melt-quenching Bi_xSe_{100-x} alloy often aid one to choose the kinetic model(s) that would actually describe its thermal stability and decomposition upon heating, so rendering an all-inclusive analysis of experimental thermoanalytical data more pragmatic, handy and timesaving.

In view of theoretical shape parameters and flow chart of Haixiang et al. (2010) and of estimated parameters (Table 2), which clarify graphical features of $\alpha(T)-T$ and $(d\alpha(T)/dT)-T$ curves of Bi_xSe_{100-x} alloys of present work, only few kinetic reaction mechanisms would embody these conversion curves and the behavior of their measured TG/DTG curves. These include the mechanism R2, described by the model function $f[\alpha(T)]=2[1-\alpha(T)]^{1/2}$ and parameters ($\alpha_m^{theor}=0.71-0.77$; $\Delta_{1/2}=14.5-72.7$) and the mechanism R3, described by the model function $f[\alpha(T)]=3[1-\alpha(T)]^{2/3}$ and parameters (T_id, T_fs; $\alpha_m^{theor}=0.58\sim0.70$; $\Delta_{1/2}=16.2\sim80.3$). The first-order (n=1) reaction mechanism (F1), described by the model function $f[\alpha(T)]=[1-\alpha(T)]^{1/2}$and parameters ($T_i$d, T_fd; $\alpha_m^{theor}=0.58\sim0.70$) can be discarded on the basis of asymmetry

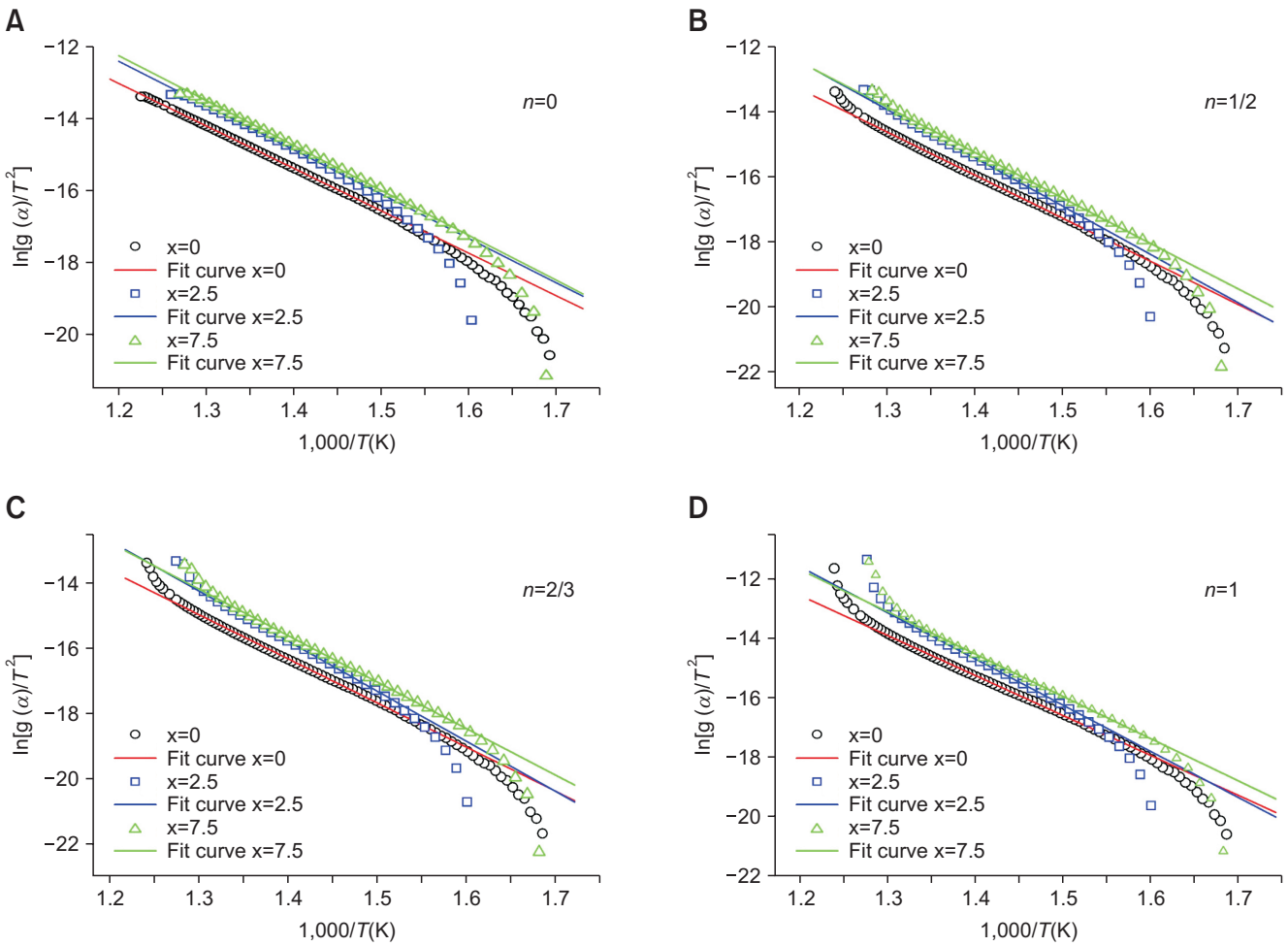

Fig. 3. The $\alpha(T)-T$(K) data calculated from the non-isothermal TG data measured at β=10 K/min for the three powder samples Bi_0Se_{100}, $Bi_{2.5}Se_{97.5}$ and $Bi_{7.5}Se_{92.5}$ (A) n=0, (B) n=1/2, (C) n=2/3, and (D) n=1. This data is plotted on basis of CR method and nth-order model function $f[\alpha(T)]=\gamma[1-\alpha(T)]^n$ as $\ln\{g[\alpha(T)]/[T(K)]^2\}$-Vs-1,000/$T$(K). The function $g[\alpha(T)]\{=-\ln[1-\alpha(T)]\}$ and $g[\alpha(T)]=[1-[1-\alpha(T)]^{1-n}]/(1-n)$. Solid lines are linear regression fits to linear portions, and dashed curves are guides-to-eye.

Table 3. Parameters of Kinetic reaction mechanisms for functions $f[\alpha(T)]=\gamma[1-\alpha(T)]$ (n=0, 1/2, 2/3, 1), deduced from best fits of $\alpha(T)$-T and $d\alpha(T)/dt$-T conversion curves of studied Bi_xSe_{100-x} samples to the ABS and CR kinetic formulas. Best curve fits of the data of undoped selenium sample to ABS formula were made for $0.02<\alpha(T)<0.45$

Analysis method	Sample	Reaction order							
		E_α (kJ/mol)	A (min^{-1})	E_α (kJ/mol)	A (min^{-1})	E_α (kJ/mol)	A (min^{-1})	E_α (kJ/mol)	A (min^{-1})
		n=0		n=1/2		n=2/3		n=1	
CR	Bi_0Se_{100}	97.9	3.5×10^5	104.6	6.0×10^5	106.6	5.9×10^5	107.6	2.2×10^6
	$Bi_{2.5}Se_{97.5}$	102.2	1.3×10^6	117.1	9.3×10^6	121.0	1.3×10^7	124.2	7.0×10^7
	$Bi_{7.5}Se_{92.5}$	103.6	1.8×10^6	110.3	3.3×10^6	112.3	3.2×10^6	113.8	1.3×10^7
ABS	Bi_0Se_{100}	96.0	3.3×10^9	100.5	4.0×10^9	103.2	4.5×10^9	108.2	3.6×10^{10}
	$Bi_{2.5}Se_{97.5}$	99.7	1.1×10^{10}	108.1	2.9×10^{10}	110.0	2.7×10^{10}	114.1	1.9×10^{11}
	$Bi_{7.5}Se_{92.5}$	97.3	8.1×10^9	100.7	8.1×10^9	100.9	5.6×10^9	103.5	2.9×10^{10}

(shape) factor S>1, as was found for our Bi_xSe_{100-x} alloys. The zero-order (n=0) reaction mechanism (R0), described by the model function $f[\alpha(T)]$=1 was not treated by Shape methods and is not included in the scheme of the currently-used flow charts (Gao et al., 1993; Haixiang et al., 2010; Lee & Dollimore, 1998) and no theoretical shape parameters for the R0 mechanism are yet available, though its model function was used to analyze experimental data of thermally-induced decomposition of some materials (Marini et al., 1979).

To distinguish between above-stated kinetic reaction mechanisms, and identify which one is suitable for describing thermal decomposition of studied Bi_xSe_{100-x} alloys, we shall perform curve-fitting of their $\alpha(T)-T$ and $(d\alpha(T)/dT)-T$ data to model-based differential-form ABS and integral-form CR methods on using the nth-order model functions. Quantitative analysis of the $\alpha(T)-T$(K) and $(d\alpha(T)/dT)-T$ data of Bi_xSe_{100-x} powder samples were also made for kinetic reaction mechanism F1, whose theoretically shape factor is 1 (Haixiang et al., 2010), though it can be discarded by S>1 determined for these samples.

Quantitative Analysis of Experimental TG/DTG Data

Quantitative analysis of the $\alpha(T)-T$(K) and $(d\alpha(T)/dT)-T$(K), constructed from TG/DTG curves of the melt-quenching Bi_xSe_{100-x} samples (x=0, 2.5, and 7.5 at%) obtained for β=10°C/min has been performed on the basis of the model-based differential-form ABS (Eq. (3)) and integral-form CR formulas (Eq. (4)). This analysis was implemented by making use of the nth-order function $f[\alpha(T)]\propto[1-\alpha(T)]^n$ and its function $g[\alpha(T)]$ given in Eq. (5), which model the kinetic reaction mechanisms R0 (n=0), R2 (n=1/2), R3 (n=2/3) and F1 (n=1). In TG terminology, the reaction conversion factor $\alpha(T)$ is the fraction of sample decomposed at the temperature T (fractional decomposition), calculated for a specific range, where a kinetic reaction mechanism is operative. Fig. 3 depict the calculated data $\alpha(T)-T$(K) of our Bi_0Se_{100}, $Bi_{2.5}Se_{97.5}$ and $Bi_{7.5}Se_{92.5}$ powder samples as plots of $\ln\{g[\alpha(T)]/[T(K)]^2\}$-Vs-[1,000/$T$(K)] on the basis of the CR-formula expressed in Eq. (3), using the functions $g[\alpha(T)]$ for the model functions $f_0[\alpha(T)]=1$, $f_{1/2}[\alpha(T)]=2[1-\alpha(T)]^{1/2}$, $f_{2/3}[\alpha(T)]=3[1-\alpha(T)]^{2/3}$, and $f_1[\alpha(T)]=[1-\alpha(T)]$ describing the R0, R2, R3 and F1 kinetic reaction mechanisms, respectively. These plots show that the application of CR method to analyze the non-isothermal $\alpha(T)-T$(K) data of the studied Bi_xSe_{100-x} samples gives curvilinear trends for the R2-, R3- and F1-model functions over a good part of the $\alpha(T)$-values of the decomposition process. Yet, analysis of same $\alpha(T)-T$(K) data on basis of model-based integral-form CR formulation and model function of kinetic reaction mechanism R0 (n=0), for which $g[\alpha(T)]=\alpha(T)$, yields wider linear portions on plots of Fig. 3 with the best linear fits over a quite broad $\alpha(T)$-range. Table 3 lists the values of activation energy E_α and frequency factor A determined from attained linear fits on Fig. 3.

The R0 kinetic reaction mechanism appears to correspond to a linear variation of $\alpha(t)$ with the time t in the isothermal mode (Marini et al., 1979) and seems to account for the observed thermal decomposition of our Bi_xSe_{100-x} powder samples over fairly wide range of $\alpha(T)$-values. The curvilinear trend seen on the $\ln\{g[\alpha(T)]/[T(K)]^2\}$-Vs-[1,000/$T$(K)] plots fitted to the CR formula can be attributed to setting T_0, the lower temperature limit of the integral of Eq. (4) to zero, an assumption that is not always adequate. To remove the non-linearity of the plots attained on the basis of the model-based integral form CR kinetic analysis method, T_0 should be chosen to be a non-zero finite temperature at which the process of thermal decomposition of a heated sample actually starts (Marini et al., 1979). This amendment and its consequence implications on the analysis of as-measured TG curves of Bi_xSe_{100-x} powder samples will be conducted in a forthcoming article, as a preliminary analysis of the $\alpha(T)-T$ curves on the basis of the modified formulations of RC formula gave remarkable non-linear curve-fits over much broader $\alpha(T)$-range.

On the other hand, the calculated $(d\alpha(T)/dT)-T$(K) data of the studied Bi_xSe_{100-x} powder samples were analyzed on the basis of the linear formulation of the model-based

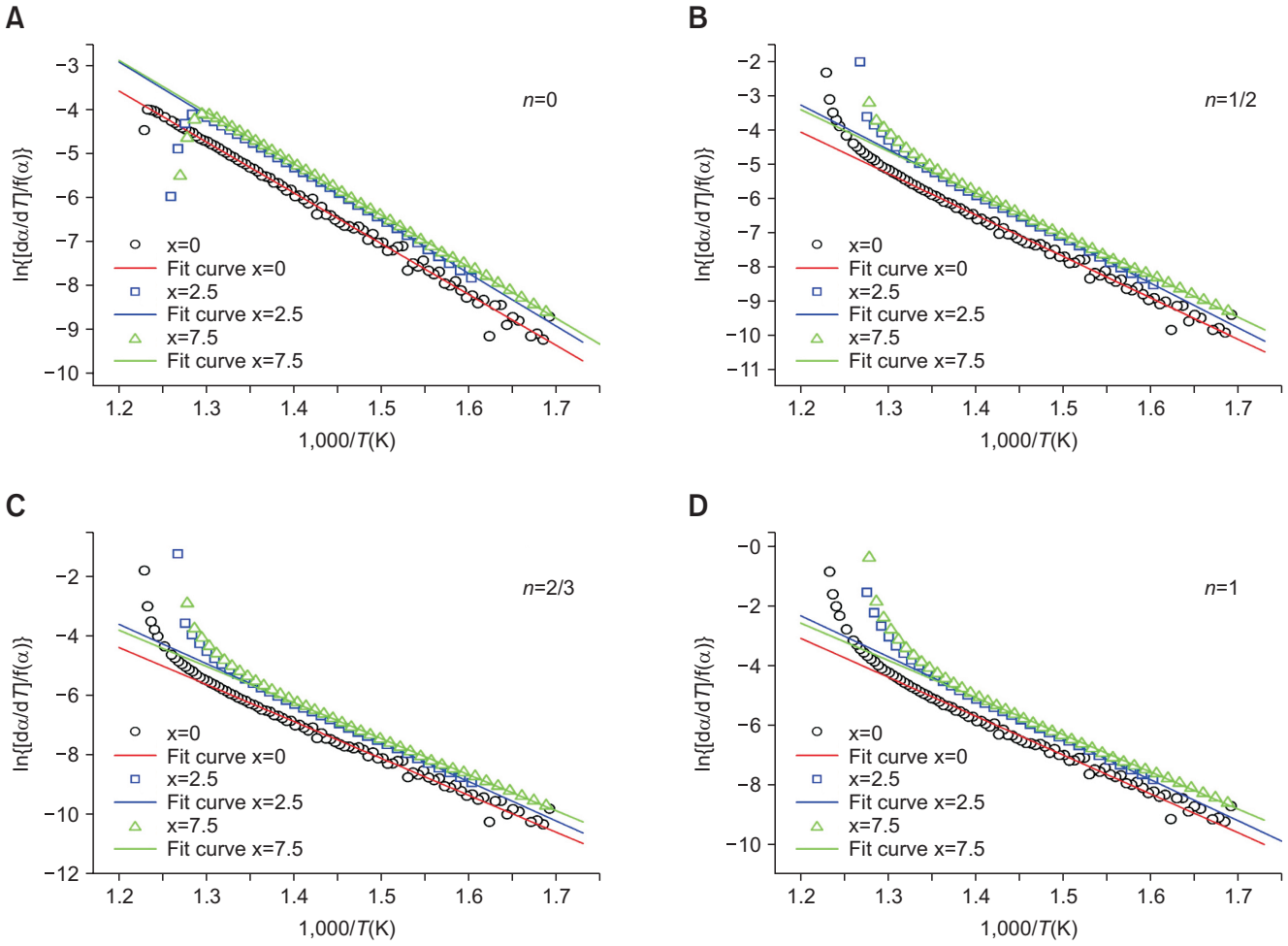

Fig. 4. The (d$\alpha(T)$/dT)–T(K) data calculated from non-isothermal thermogravimetry (TG) data measured at β=10 K/min for the samples Bi_0Se_{100}, $Bi_{2.5}Se_{97.5}$ and $Bi_{7.5}Se_{92.5}$. (A) n=0, (B) n=1/2, (C) n=2/3, and (D) n=1. The data is plotted on basis of ABS method and the nth-order model function $f[\alpha(T)]=\gamma[1-\alpha(T)]^n$ as ln{[d$\alpha(T)$/dT]/$f[\alpha(T)]$}-Vs-1,000/T(K). The function $g[\alpha(T)]=-\ln[1-\alpha(T)]$ and $g[\alpha(T)]=[1-[1-\alpha(T)]^{1-n}]/[(1-n)]$. Dotted lines are linear regression fits to linear portions, and solid curves are guides-to-eye.

differential-form ABS method exemplified in Eq. (3), along with the model function $f[\alpha(T)]=\gamma[1-\alpha(T)]^n$ describing the kinetic reaction mechanisms R0 (n=0; γ=1), R2 (n=1/2; γ=2), R3 (n=2/3; γ=3) and F1 (n=1; γ=1). Fig. 4 depict the resulting representation depicted as plots of ln{[d$\alpha(T)$/dT]/$f[\alpha(T)]$}-Vs-[1,000/T(K)] for the respective n values, which exhibit narrow linear portions over a limited range of $\alpha(T)$-values; however, the much longer linear portion and the best linear fit are noted to be assigned with the kinetic reaction mechanism R0 (n=0) for values of $\alpha(T)$ covering a rather wide range of $\alpha(T)$ ($0.02<\alpha(T)<0.8$). The values of the activation energy E_α and frequency factor A determined from linear fits on Fig. 4 are also listed in Table 3.

CONCLUSIONS

Detailed non-isothermal TG measurements on small masses (~13 mg) of several melt-quenched Bi_xSe_{100-x} powder samples (x=0, 2.5, and 7.5 at%) were taken at a constant heating rate β=10°C/min in the temperature range 35°C~950°C. The as-measured TG curves illustrate good thermal stability of samples with no loss of their initially-used masses at temperatures less than T≈400°C, above which mass loss starts to greatly decrease up to 600°C. Between 600°C and 950°C, trivial mass loss is observed and the residual mass left behind is related to the Bi-content in the used powder sample. Presuming that a melt-quenching Bi_xSe_{100-x} sample decomposes into its ingredients, the as-measured TG curves were used to estimate its molar (Se/Bi)-ratio; however, these calculations were not in accord with the molar ratios of bismuth and selenium powders mixed together in the preparation of their original Bi_xSe_{100-x} alloys.

The graphical features of the shape of conversion curves of Bi_xSe_{100-x} samples, combined with a flow chart help to

reduce the many kinetic reaction mechanisms causing their thermal decomposition to few ones, namely the R2, R3 and F1 kinetic reaction mechanisms, described by the nth-order model function $f[\alpha(T)] \propto [1\text{-}\alpha(T)]^n$ (n=1/2, 2/3, and 1). To discriminate between these models and elucidate which one is suitable to account for decomposition of Bi_xSe_{100-x} samples, the $\alpha(T)$–T and $(d\alpha(T)/dT)$–T data were analyzed by the model-based integral CR and differential ABS kinetic formulas, combined with these model functions, but linearity of plots were only achieved in a limited range of $\alpha(T)$-values. Yet, it was found that analyzing such conversion curves by the CR and ABS methods using the model function of kinetic reaction mechanism R0 (n=0) (Marini et al., 1979) gave remarkable linear fits over much broader $\alpha(T)$-range.

CONFLICT OF INTEREST

No potential conflict of interest relevant to this article was reported.

REFERENCES

Abdel-Rahim M M, El-Korashy A, Hafiz M M, and Mahmoud A Z (2008) Kinetic study of non-isothermal crystallization of Bi_xSe_{100-x} chalcogenide glasses. *Physica B* **403**, 2956-2962.

Abu El-Oyoun M (2000) Crystallization kinetics of the chalcogenide $Bi_{10}Se_{90}$ glass. *J. Phys. Chem. Sol.* **61**, 1653-1662.

Achar B N N, Brindley G W, and Sharp J H (1966) Kinetics and mechanism of dehydroxylation processes; III, Applications and limitations of dynamic method. *Proceedings of International Clay Conference, Jerusalem* **1**, 67-73.

Ahmad M J A (2016) Study of structural and optical properties of bismuth-doped selenium films prepared by flash-evaporation method. M.Sc. thesis (The University of Jordan, Jordan).

Atmani H (1988) Glass transition study of Bi_xSe_{1-x} materials. *Mater. Chem. Phys.* **19**, 235-242.

Atmani H (1992) Some aspects of the behavior of Bi in a matrix of Se. *Mater. Lett.* **13**, 21-26.

Atmani H, Coquerel G, and Vautier C (1989) Crystallization and melting of thin Bi_xSe_{1-x} layers. *Thin Solid Films* **177**, 239-244.

Atmani H and Vautier C (1989) Bismuth effects on crystallization of amorphous selenium. *Mater. Chem. Phys.* **23**, 541-550.

Bettsteller R, Witte H, Herms W, and Freistedt H (1993) Influence of Bismuth Incorporation on the Optical properties of a-Se Films. *Solid State Commun.* **87**, 763-765.

Brown M E (2004) *Introduction to Thermal Analysis: Techniques and Applications* (Kluwer Publishers, London).

Chen Y, Liu Y, Chu M, and Wang (2014) Phase diagrams and thermodynamic descriptions for the Bi-Se and Zn-Se binary systems. *J. Alloys. Comp.* **617**, 423-428.

Coat A W and Redfern J P (1964) Kinetic parameters from thermogravimetric data. *Nature* **201**, 68-69.

Criado J M, Málek J, and Ortega A (1989) Applicability of the Master plots in kinetic analysis of non-isothermal data. *Thermochimica Acta* **147** 377-385.

Dollimore D, Evans T, Lee Y, Pee G, and Wilburn F (1992a) The significance of the onset and final temperatures in the kinetic analysis of TG curves. *Thermochimica Acta* **196**, 255-265.

Dollimore D, Evans T A, Lee Y F, and Wilburn F W (1992b) Correlation between the shape of a TG/DTG curve and the form of the kinetic mechanism which is applying. *Thermochimica Acta* **198**, 249-257.

Flynn J H and Wall L A (1966) A quick, direct method for the determination of activation energy from thermogravimetric data. *J. Polymer Sci.: Part B. Polymer Lett.* **4**, 323-328.

Gao X, Chen D, and Dollimore D (1993) The correlation between the value of α at the maximum reaction rate and the reaction mechanisms. A theoretical study. *Thermochimica Acta* **223**, 75-82.

Hafiz M M, El-Shazly O, and Kinawy N (2001) Reversible phase in BixSe100-x chalcogenide thin films for use as optical recording medium. *Appl. Surf. Sci.* **171**, 231-241.

Haixiang C, Naian L, and Weitao Z (2010) Critical study on the identification of reaction mechanism by the shape of TG/DTG curves. *Solid State Sci.* **12**, 455-460.

Innami T and Adachi S (1999) Structural and optical properties of photocrystallized Se films. *Phys. Rev. B* **328**, 8284-8289.

Jafar M M Abdul-Gader, Saleh M H, Ahmad M J A, Bulos B N, and Al-Daraghmeh T M (2016) Retrieval of optical constants of undoped amorphous selenium films from an analysis of their normal-incidence transmittance spectra using numeric PUMA method. *J. Mater. Sci: Mater. Electron.* **27**, 3281-3291.

Jenkins R (1999) *X-Ray Fluorescence Spectrometry, Vol. 2* (Wiley & Sons, New York).

Jones L F, Dollimore D, and Nicklin T (1975) Comparison of experimental kinetic decomposition data with master data using a linear plot method. *Thermochimica Acta* **13**, 240-245.

Kasap S O, Aiyah V, and Yannacopoulos S (1990) Thermal and mechanical properties of amorphous selenium films in the glass transformation region. *J. Phys. D: Appl. Phys.* **23**, 553-556.

Kasap S O and Rowlands J A (2000) X-ray photoconductors and stabilized a-Se for direct conversion digital flat-panel X-ray image detectors. *J. Mater. Sci: Mater. Electron.* **11**, 179-198.

Keattch C J and Dollimore D (1975) *An Introduction to Thermogravimetry, Vol. 2* (Heyden, London).

Kotkata M F, Abdel-Wahab F A, and Al-Kotb M S (2009) Effect of In-content on the optical properties of a-Se films. *Appl. Surf. Sci.* **255**, 9071-9077.

Lee Y F and Dollimore D (1998) The identification of the reaction mechanism in rising temperature kinetic studies based on the shape of the DTG curve. *Thermochimica Acta* **323**, 75-81.

Marini A, Berbenni V, and Flor G (1979) Kinetic parameters from

thermogravimetric data. *Z. Naturforsch.* **34a**, 661-663.

Mehra R M, Kaur G, Pundir A, and Mathur P C (1993) Study of Se-Te-Sb system for application to reversible optical-data storage. *Jpn. J. Appl. Phys.* **32**, 128-129.

Mehta N (2006) Applications of chalcogenide glasses in electronics and optoelectronics: a review. *J. Sci. Ind. Res.* **65**, 777-786.

Moharram A H and Abu El-Oyoun M (2000) Pre-crystallization kinetics of the $Bi_{10}Se_{90}$ glass. *J. Phys. D: Appl. Phys.* **33**, 700-703.

Mott N F and Davis E A (1979) *Electronic Processes in Non-Crystalline Materials* (Oxford University, Oxford).

Moukhina E (2012) Determination of kinetic mechanisms for reactions measured with thermoanalytical instruments. *J. Therm. Anal. Calorim.* **109**, 1203-1214.

Okamoto H (1994) The Bi-Se (Bismuth-Selenium) system. *J. Phase Equilibria* **15**, 195-201.

Ozawa T (1965) A new method of analyzing thermogravimetric data. *Bulletin Chem. Soc. Jpn.* **38**, 1881-1886.

Perez-Maqueda L A, Ortega A, and Criado J M (1996) The use of master plots for discriminating the kinetic model of solid state reactions from a single constant-rate thermal analysis (CRTA) experiment. *Thermochimica Acta* **277**, 165-173.

Ptáček P, Kubátová D, Havlica J, Brandštetr J, Šoukal F, and Opravil T (2010) The non-isothermal kinetic analysis of the thermal decomposition of kaolinite by thermogravimetric analysis. *Powder Technol.* **204**, 222-227.

Saleh M H, Ershaidat N M, Ahmad M J A, Bulos B N, and Jafar M M Abdul-Gader (2017) Evaluation of spectral dispersion of optical constants of a-Se films from their normal-incidence transmittance spectra using Swanepoel algebraic envelope approach. *Opt. Rev.* **24**, 260-277.

Saxena M and Bhatnagar P K (2003) Crystallization study of Te-Bi-Se glasses. *Bull Mater. Sci.* **26**, 547-551.

Šesták J (1984) Thermal Analysis, Part D: *Thermophysical Properties of Solids, Their Measurements and Theoretical Thermal Analysis* (Elsevier, Amsterdam).

Sharp H K, Brindley G W, and Achar B N N (1966) Numerical data for some commonly used solid state reaction equations. *J. Am. Ceram. Soc.* **49**, 379-382.

Sharp J H and Wentworth SA (1969) Kinetic analysis of thermogravimetric data. *Anal. Chem.* **41**, 2060-2062.

Tichy L, Ticha H, Triska A, and Nagels C (1985) Is the n-type conductivity in some Bi-doped chalcogenide glasses controlled by percolation? *Solid State Commun.* **53**, 399-402.

Tonchev D and Kasap S O (2002) Effect of ageing on glass transformation measurements by temperature modulated DSC. *Mater. Sci. Eng. A* **328**, 62-66.

van der Heide P (2012) *X-ray Photoelectron Spectroscopy: An Introduction to Principles and Practices* (Wiley, Hoboken).